Three-phase Active and Reactive Power Control in Home Energy Management System

Bharath Varsh Rao and Friederich Kupzog
Electric Energy Systems – Center for Energy
AIT Austrian Institute of Technology
1210 Vienna, Austria
{bharath-varsh.rao, friederich.kupzog}@ait.ac.at

Martin Kozek
Institute of Mechanics and Mechatronics
Vienna University of Technology
1060 Vienna, Austria
martin.kozek@tuwien.ac.at

***Abstract*—This paper presents a three-phase unbalanced home energy management system which generates both active and reactive power control set-points for various flexibilities in smart home. In recent years, number of smart energy homes consisting of distributed energy resources like photo-voltaic systems, micro-wind, new loads like electric storage, heat-pumps and controllable loads have increased. They are directly influenced by various external disturbances and is essential to optimally manage them to get a system level optimization. Additionally, these devices are single or three phased in nature, adding to the complexity. Models and control structure associated with these flexibilities need to be sufficiently accurate to capture its entire behavior. To do so, the authors have presented a three phase unbalanced home energy management system which uses a nonlinear-non-convex model predictive control. Three conflicting objective functions, maximization of user comfort, self-consumption and grid support is presented. This control structure is applied to a real smart home in Austria and the simulation results are provided.**

***Index Terms*—Home Energy Management System, Three-phase Unbalance, Non-linear, Non-convex, Model Predictive Control.**

I. Introduction

In the context of smart cities and low voltage distribution networks, the nature of loads has changed over the years. New loads like heat-pumps, electric storage and vehicles, are being increasingly connected. Additionally, with the introduction of distributed energy resources (DER's) like photo-voltaic systems, micro-wind and hydro, it is harder to manage the grid in a secure fashion. These devices are single or three phased in nature and the models currently representing them are not sufficient enough to incorporate this complexity.

Since largest share of energy production, in the near future, is expected to be consumed by homes and buildings in cities, it is essential to manage them in an optimal fashion to increase grid resilience and economic benefit for the consumer. The focus of research work presented in this paper is to optimally schedule the flexibilities in a smart home according to three objective functions. Based on the nature of various controllable devices, referred to flexibilities, and the involvement of external disturbances, model predictive control (MPC) with receding horizon control is used.

In the literature, various implementations of MPC applied to smart homes are available. In [1], a MPC scheme to perform load shifting for various household devices like energy storage. The objective function is to minimize daily energy cost using demand response, time of use tariff and the devices are scheduled based on it. Authors in [2] present a methodology to generate optimal schedules using MPC for various flexibilities in smart building. It uses real-time pricing to schedule thermal and non-thermal units by taking into account the disturbance forecasts and thermal parameters of the building. The objective is to minimize energy consumption. A nonlinear MPC is implemented in [3] to schedule heat recovery ventilators using reduced-order models from single-zone test building. The goal of the controller is to minimize energy consumption. In [4], a MPC scheme to control room temperature and simple models to include air conditioning, humidity and living appliances to get a complete model of the room. Additionally, photo-voltaic system, wind generators were included. In [5], objectives of the controller is to minimize energy consumption and maximize user comfort. The controller used is an MPC compute future room temperature, illumination and position of window blinds by considering various disturbances. The user is given a choice to choose their comfort level based on three predetermined values. Simulation is done for winter and summer days to get results for total building energy consumption. Authors in [6], a demand response strategy in HEMS in the context of smart grids is presented. It is used to reduce total energy costs along with the revenue generated by performing demand side management using electric storage.

Heating, ventilation and air conditioning systems, known as HVAC, control schematic is presented in [7]. MPC is used to optimally operate these devices in building and help them participate in the market to provide demand response. Simulations are performed using price signals and results of their behavior is presented. In [8], two level control strategy is presented. It involves a upper level which optimizes energy optimal control, while the lower level controller deal with individual subsystems. Focus of the research in [9] is to obtain the impact of MPC in building energy savings along with local DER productions. Three scenarios, on-peak, mid-peak and off-peak hour loading is utilized to generate optimal schedules. In [10], a detailed comparison between on-off thermostat control, PID control and MPC is presented. It is used to control domestic heaters and air-conditioning system to get maintain the temperature of a room within its limits. It is also used to maximize economic benefit using time of use tariff. Authors in [11], have proposed an Economic MPC for a group of buildings to share heat-pumps and get a system level optimization. It shows a 15% reduction in energy usage when compared to the buildings

optimizing on their own.

This paper, is an extension of work done in [12] where, three phase unbalanced home energy management system is presented. The authors present various linear models for flexibilities which are single or three phased in nature. The major limitation was the linear implementation of three phase electric storage and inverter connected to it. Model of electric storage uses one efficiency for both charging, discharging cycles and inverter is simplified to operate at unity power factor. Doing so, mitigates the reactive power control as inverter is the only device which can be used to control it directly and devices like heat-pumps and controllable loads operate at constant power factor.

In this paper, the above mentioned issues are addressed by considering complete inverter and electric storage formulation leading to non-linear and non-convex problem. A three phase unbalanced home energy management system using non-linear non-convex models predictive control using distributed genetic algorithm.

The following contributions are presented in this paper.

1) Comprehensive modelling of hybrid system consisting of thermal model of smart home physical structure, electrical models of various single and three phase appliances like heat pump (connecting thermal and electrical models), controllable and uncontrollable loads, photovoltaic systems, inverter connected to electric storage.
2) Non-linear electric storage and inverter models to include reactive power control.
3) Non-linear non-convex Model Predictive Control for Home Energy Management System.
4) Model Predictive Control applied to a real home in Austria.

II. System Models

With the increase in flexibilities connected to smart homes in low voltage distribution networks, it is essential to model them appropriately to accommodate various key characteristic features capturing the main dynamics. Smart homes are hybrid systems consisting of thermal and electrical components, coupled only by a heat-pump. In this section, models of these flexibilities are presented.

A. Thermal Models

Thermal models of smart home are presented in this section. It consists of home physical structure (wall, floor, ceiling and room temperatures) and heat-pump models.

1) Thermal Structure: Linear thermal models are based on single zone non-linear models developed using data from real homes located in cities of Vienna and Salzburg in Austria. The data was clustered and consolidated into four use-cases representing typical homes from the region are considered in this paper and their key parameters like control method, rated capacities and heat demand are tabulated in Table I. These models were generated and acquired from project iWPP-Flex [**?**].

Thermal models of smart homes are kept sufficiently simple to increase generality since it must be used widely in the region. Therefore, first order continuous state-space models are implemented, and then discretized with 15 min sampling time, presented in Equation 1.

$$x_{room}(t+1) = A_{room}\, x_{room}(t) + B_{room}\, u_{room}(t) \quad (1)$$

Where, x_{room} represents the state variables consisting of wall and room temperatures. Wall temperature is walls, ceiling and floor (Building structure) net temperatures. The system matrices are represented using A_{room} and B_{room}.

$$x_{room} = \begin{bmatrix} T_{wall} \\ T_{room} \end{bmatrix} \quad (2)$$

Equations 3 and 4 presents the limits on room and wall temperatures.

$$T_{wall}^{min} \leq T_{wall}(t) \leq T_{wall}^{max} \quad (3)$$

$$T_{room}^{min} \leq T_{room}(t) \leq T_{room}^{max} \quad (4)$$

Input vector u_{room} is presented in Equation 5. It consists of heat flow supplied into the home using a heat-pump, ambient temperature, irradiation, internal gains, and ventilation losses.

The input quantities for the building are heat flow supplied by the heat pump, ambient temperature, solar irradiation from all directions, internal gains, and ventilation.

$$u_{room} = \begin{bmatrix} q_{room} \\ T_{ambient\,temperature} \\ i_{north} \\ i_{east} \\ i_{south} \\ i_{west} \\ g_{internal\,gain} \\ g_{ventilation} \end{bmatrix} \quad (5)$$

Equation 6 presents limits on heat flows. Since only heating is involves, q_{room} is positive.

$$0 \leq q_{room}(t) \leq q_{room}^{max} \quad (6)$$

2) Heat Pump in Residential Building: As discussed in Section II-A, heat-pump is the only component coupling both thermal and electrical parts of the system. It is used to supply heat flows into the home. The relationship between heat-pump active power $P_{heat\,pump}$ and heat flows q_{room} is presented in Equation 7. For the sake of simplicity, it uses constant coefficient-of-performance (*cop*) throughout the year. This equation represents only a single-phase heat-pump. To get three phase models, right-hand side of Equation 7 is divided by three to with equal powers distributed over three phases.

$$P_{heat\,pump}(t) = \frac{q_{room}(t)}{cop_{heat\,pump}} \quad (7)$$

Where, active power and cop are $P_{heat\,pump}$ and $cop_{heat\,pump}$ respectively. A binary variable $B_{heat\,pump}$ is used to model Low-energy and existing house since they contain on/off heat-pump.

$$P_{heat\,pump}(t) = B_{heat\,pump}\, P_{heat\,pump}^{rated} \quad (8)$$

TABLE I
VARIOUS KEY PARAMETERS OF FOUR TYPICAL HOMES IN AUSTRIA.

House Hype	Passive House	Low-Energy House	Existing House	Renovated House
Heating demand	15 $kWh/(m^2a)$	45 $kWh/(m^2a)$	100 $kWh/(m^2a)$	75 $kWh/(m^2a)$
Heater	Under floor	Under floor	Radiator	Radiator
Heat exchange medium	Air-water	brine-water	brine-water	air-water
Power control	Variable	On/off	On/off	Variable
Rated capacity (Electrical / thermal)	1 kW/ 3 kW	1.2 kW/5 kW	5 kW/12kW	2.7 kW/7 kW

The heat-pump motor is operated at constant power factor ($pf_{heat\,pump}$) leading to Equation 9.

$$Q_{heat\,pump}(t) = tan(cos^{-1}(pf_{heat\,pump}))P_{heat\,pump}(t) \tag{9}$$

Only heating period is considered and therefore, $P_{heat\,pump}$ and $Q_{heat\,pump} \geq 0$. The following are the limits on heat pump active power limits.

$$0 \leq P_{heat\,pump}(t) \leq P^{max}_{heat\,pump} \tag{10}$$

Heat pump reactive power limits are presented below,

$$0 \leq Q_{heat\,pump}(t) \leq Q^{max}_{heat\,pump} \tag{11}$$

Maximum rated active and reactive powers of head pump are $P^{max}_{heat\,pump}$ and $Q^{max}_{heat\,pump}$ respectively.

B. Electrical System

This section presents various models of electrical components in smart home. The models to the following flexibilities are presented in this paper.

1) Electric Storage: To maximize the use of renewable energy resources, electric storage is needed. Therefore, mixed-integer battery models are used and included in HEMS. Energy balance is presented in Equation 12. The charging and discharging powers are split into two variables. This is done to have more accurate storage model with both charging and discharging efficiencies making it nonlinear. To deal with this, a binary variable, $B_{battery}$ is introduced, making the problem, mixed-integer and linear.

$$\begin{aligned} &soc(t+1)\, C_{battery} = soc(t)\, C_{battery} \\ &+ B_{battery}(t)\, \eta_{charging\,efficiency}\, P_{battery\,charging}(t) \\ &- (1 + B_{battery}(t))\, \frac{P_{battery\,discharging}(t)}{\eta_{discharging\,efficiency}} \end{aligned} \tag{12}$$

Where, $C_{battery}$ is the capacity. $P_{battery\,charging}$ and $P_{battery\,discharging}$, are charging and discharging power respectively coupled with $\eta_{charging\,efficiency}$ and $\eta_{discharging\,efficiency}$, charging and discharging efficiencies.

Constraints on limits of soc is as follows.

$$soc^{min} \leq soc(t) \leq soc^{max} \tag{13}$$

Constraints on limits on battery charging and discharging power are as follows.

$$P^{min}_{battery} \leq P_{battery\,charging}(t) \leq 0 \tag{14}$$

$$0 \leq P_{battery\,discharging}(t) \leq P^{max}_{battery} \tag{15}$$

C. Three-Phase Inverter

Three phase inverter in this paper is used to control active and reactive powers on each of the three phases. This is very helpful for example, to balance the three phases. The battery from previous section is connected to this inverter. The relationship between them is described using power balance Equations 16 and 17.

$$\begin{aligned} (S_{inverter\,infeed}(t))^2 =& (P_{inverter\,infeed}(t))^2 \\ &+ (Q_{inverter\,infeed}(t))^2 \end{aligned} \tag{16}$$

Single the battery power is divided into charging and discharging powers, same is done for the inverter.

$$\begin{aligned} (S_{inverter\,consumption}(t))^2 =& (P_{inverter\,consumption}(t))^2 \\ &+ (Q_{inverter\,consumption}(t))^2 \end{aligned} \tag{17}$$

Since battery can only provide active power, Equations 18 and 19 are introduced. Reactive power can be absorbed or injected by semiconductors switched in the inverter.

$$P_{battery\,discharging}(t) = P_{inverter\,infeed}(t) \tag{18}$$

$$P_{battery\,charging}(t) = P_{inverter\,consumption}(t) \tag{19}$$

Where, $\mathfrak{p} \in phases(r, s, t)$. Equation 16 and 17 are nonlinear and non-convex in nature along with the binary variables from Section II-B1. Contrary to the implementation in [12], in this paper, full control on per-phase active and reactive powers are provided.

The relationship between per-phase active and reactive powers are described in Section 20 and 21.

$$P_{inverter}(t) = \sum_{\mathfrak{p}} P^{\mathfrak{p}}_{inverter}(t) \tag{20}$$

$$Q_{inverter}(t) = \sum_{\mathfrak{p}} Q^{\mathfrak{p}}_{inverter}(t) \tag{21}$$

D. Controllable Loads

Controllable loads are used as dump loads, described in Equation 22. Reactive power is defined using constant power factor, described in Equation 24.

Constraints on limits of controllable load active and reactive powers are as follows.

$$0 \leq P^{\mathfrak{p}}_{controllable\,load}(t) \leq P^{max}_{controllable\,load} \tag{22}$$

$$0 \leq Q^{\mathfrak{p}}_{controllable\,load}(t) \leq Q^{max}_{controllable\,load} \tag{23}$$

Power factor is assumed to be constant and is typically between 0.90 to 0.95.

$$Q^{\mathfrak{p}}_{controllable\,load}(t) = tan(cos^{-1}(pf_{controllable\,load})) \\ P^{\mathfrak{p}}_{controllable\,load}(t) \tag{24}$$

E. Grid Connection Point

Smart homes are connected to the grid at grid-connection-point (point of common coupling). Limits on active and reactive powers at the grid connection point, are presented in Equations 25 and 26.

$$P^{\mathfrak{p}}_{grid}(t) = P^{\mathfrak{p}}_{inverter}(t) + P^{\mathfrak{p}}_{heat\,pump}(t) \\ + P^{\mathfrak{p}}_{controllable\,load}(t) + P^{\mathfrak{p}}_{uncontrollable\,load} \\ + P^{\mathfrak{p}}_{photo-voltaic} \tag{25}$$

$$Q^{\mathfrak{p}}_{grid}(t) = Q^{\mathfrak{p}}_{inverter}(t) + Q^{\mathfrak{p}}_{heat\,pump}(t) \\ + Q^{\mathfrak{p}}_{controllable\,load}(t) + Q^{\mathfrak{p}}_{uncontrollable\,load} \\ + Q^{\mathfrak{p}}_{photo-voltaic} \tag{26}$$

F. Various Disturbances Applied to HEMS

Convolutional neural networks are used to forecast disturbances and more information about it is not provided in this paper. Real smart meter data from real homes is used for uncontrollable loads and photo-voltaic systems. Thermal disturbances are sourced from weather centers in Austria. Internal, ventilation losses are derived from project iWPP-Flex.

G. Objective Functions

Three conflicting objective functions are implemented in this paper. They are as follows,

1) Maximize Self-Consumption: With the increase in share of renewable energy in distribution networks, in some countries, it is more economical to self-consume. Equation 27 describes the objective for maximizing self-consumption.

$$J_{self\,consumption} = \sum_t \sum_p (P^{\mathfrak{p}}_{grid}(t))^2 \tag{27}$$

In Austria, it is more economical to feed in power into the grid. This can be easily implemented by reversing the sign of objective function at P_{grid}. The price signal is neglected for the sake of simplicity.

2) Maximize User-Comfort: User comfort is defined in Equation 28. To minimize the difference between a reference temperature trajectory and actual temperature in the room.

$$J_{user\,comfort} = \sum_t (T^{reference}_{room}(t) - T_{room}(t))^2 \tag{28}$$

3) Maximize Grid-Support: In the context of using smart homes as demand response and flexibility unit for providing grid support, the following objective in Equation 29 is introduced. It minimizes the difference between active, reactive power reference trajectories generated by a centralized controller and the actual powers at the grid connection point (see [13]). More information about the central controller is presented in [12]. The objective function on this controller is to minimize three phase unbalance at all the buses in the network.

$$J_{grid\,support} = \sum_t \sum_p (P^{\mathfrak{p}}_{grid\,reference}(t) - P^{\mathfrak{p}}_{grid}(t))^2 \\ + (Q^{\mathfrak{p}}_{grid\,reference}(t) - Q^{\mathfrak{p}}_{grid}(t))^2 \tag{29}$$

4) Complete Objective Function: By combining the three objectives, complete objective function is derived in Equation 30. User defined objective weights, $\mathfrak{S}$, $\mathfrak{U}$ and $\mathfrak{G}$ are introduced. They can be used to provide higher priority to one of the objectives. This can be done online and the effect are experienced in the very next sample time.

$$\text{minimize}\, J = \mathfrak{S}\, J_{self\,consumption} \\ + \mathfrak{U}\, J_{user\,comfort} \\ + \mathfrak{G}\, J_{grid\,support} \tag{30}$$

Controllable variables are $P^{\mathfrak{p}}_{inverter}$, $Q^{\mathfrak{p}}_{inverter}$, $P_{heat\,pump}$ and $P_{controllable\,load}$.

H. Controller

Based on the models developed in the previous section and disturbances, it can be observed that the controller needs to be robust and should be able to accommodate the daily, weekly and seasonal cycles seen in DER's, uncontrollable loads and external disturbances. The authors have chosen to use model predictive control as described in Figure 1 along with various single, three phase flexibilities and data exchanges.

Chronological sequence of control events and heuristic algorithm is based on [12].

III. Simulation and Results

MPC is simulated for the three objective functions presented in Section II-G. The three objective weights can be varied in numerous ways and therefore, four scenarios are used in this paper based on [12]. The four configurations are $\mathfrak{S}, \mathfrak{U}, \mathfrak{G}) = (0,0,1)$, $(0,1,0)$, $(1,0,0)$ and $(1,1,1)$.

The simulation parameters are presented in Table II.

The results are plotted based on each of the three objectives for a simulation horizon of 48 hours between 2019-02-1 00:00:00 and 2019-02-2 23:45:00. Active and reactive powers are presented only for phase A for the sake of simplicity.

In Figure 2, box-plot of P^A_{grid} (for phase A) is presented for various objective weights. It can be observed that for weight $(0,0,1)$, P^A_{grid} the median is equal to zero and are clustered around it. Same behavior is not seen for other weights. Although, for weight $(1,1,1)$, the MPC is not able to successfully minimize P^A_{grid} due to the existence of other objectives. In Figure 3, box-plot of $abs(T^{reference}_{room}(t) - T_{room}(t))$ for various weights is presented. It can be observed that for weight $(0,1,0)$, absolute difference between the reference and actual temperatures for the simulation horizon is minimum. The same can be observed for weight $(1,1,1)$ is due to the linear thermal model of smart home physical structure.

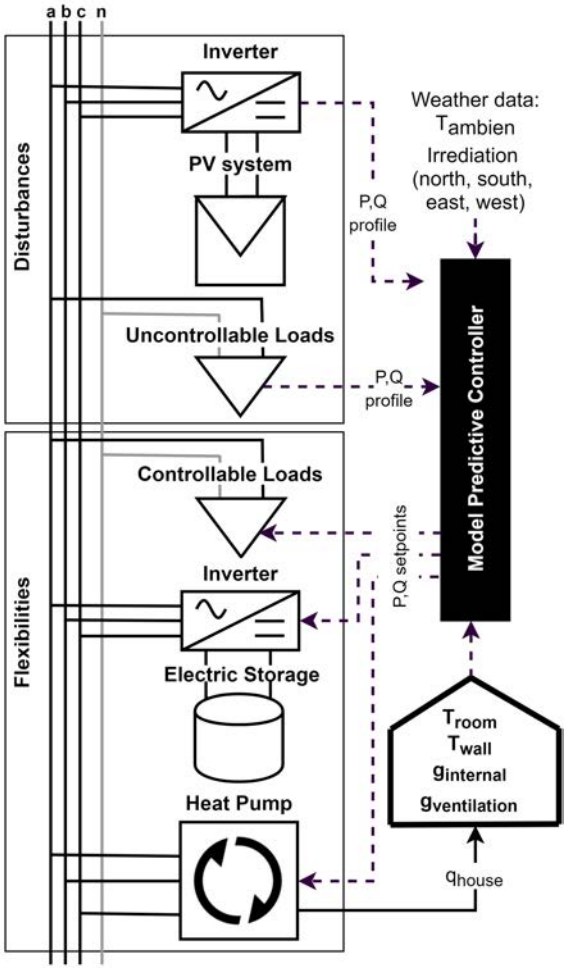

Fig. 1. Schematic of three phase home energy management system with model predictive controller.

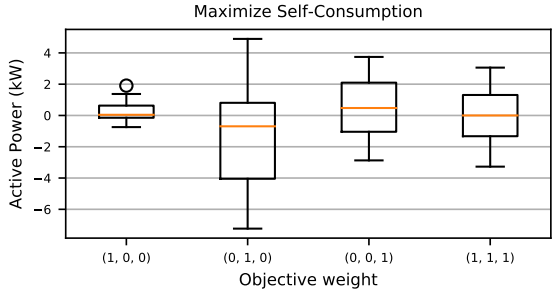

Fig. 2. Box-plot of P^A_{grid} (for phase A) for 48 hours simulation horizon for various objective weights.

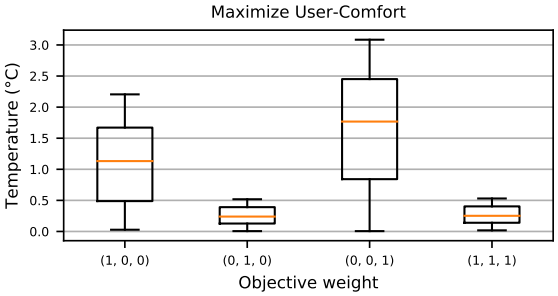

Fig. 3. Box-plot of T_{room} for 48 hours simulation horizon for various objective weights.

In Figure 4, box-plot of $abs(P^{\mathfrak{p}}_{grid\,reference}(t) - P^{\mathfrak{p}}_{grid}(t)) + abs(Q^{\mathfrak{p}}_{grid\,reference} - Q^{\mathfrak{p}}_{grid}(t)$ is presented. Similar to previous scenarios, it can be observed that for weight $(0, 0, 1)$, the objective function is minimized the most. It can also be observed that both active and reactive powers can be controlled with this MPC scheme.

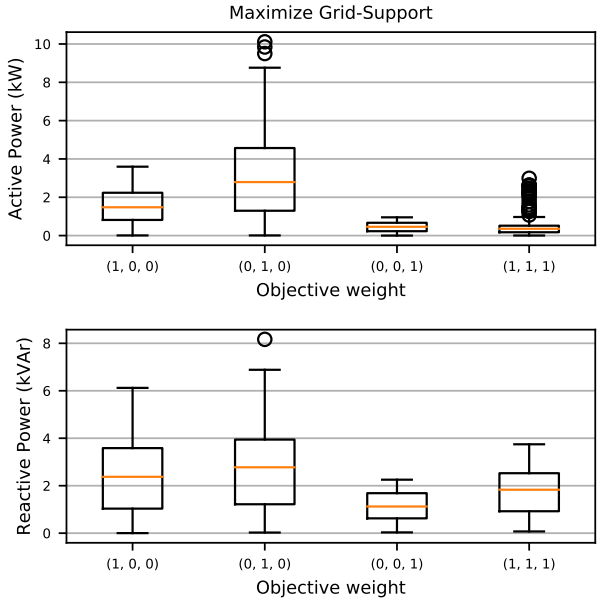

Fig. 4. Box-plot of $P^A_{grid}(t))$ and Q^A_{grid} for 48 hours simulation horizon for various objective weights.

TABLE II
MPC SIMULATION PARAMETERS

Variable	Value
Simulation parameters	
prediction horizon	24 h
control horizon	24 h
simulation duration	48 h
Building model	
T^{min}_{wall}	10 C
T^{max}_{wall}	40 C
T^{min}_{room}	18 C
T^{max}_{room}	25 C
$T_{initial}$	18 C
$T^{reference}_{room}$	20 C
Electric Storage model	
soc^{min}	0.3
soc^{max}	0.9
$C_{battery}$	20 kWh
$\eta_{battery}$	0.95
$P^{min}_{battery}$	-10 kW
$P^{max}_{battery}$	10 kW
Controllable load model	
$P^{max}_{controllable\,load}$	3 kW
$pf_{controllable\,load}$	0.95
Heat pump model	
cop	3
$pf_{heat\,pump}$	0.90
Passive house: $P^{max}_{heat\,pump}$	1 kW
Low-energy house: $P^{max}_{heat\,pump}$	1.2 kW
Existing house: $P^{max}_{heat\,pump}$	2 kW
Renovated house: $P^{max}_{heat\,pump}$	2.7 kW

IV. Conclusion

In this paper, a three phase unbalanced home energy management system using non-linear non-convex model predictive control using receding horizon control is presented. This control strategy is applied to three phase unbalanced smart home with various single and three phase flexibilities and their comprehensive models are presented. Model of a three phase unbalanced inverter with its non-convex formulation is implemented and used to provide per-phase active and reactive power control. Three conflicting objective functions, to maximize self consumption, user comfort and grid support are provided. Simulation results suggests that, using flexibilities, per phase active and reactive control can be achieved. Results for various objective functions, based on their control weights are presented.

In the future work, realistic nonlinear smart home thermal models need to be incorporated. Smart home models are single zone, which needs to be extended to the entire house by considering heat flows between various rooms. Additionally, flexibility models like uncontrollable loads and heat-pumps use constant power factors, which in reality are varying. This is also applicable to coefficient-of-performance which is assumed to constant in this paper.

Acknowledgment

The authors would like to thank the members of Power System Digitalization group of Electric Energy Systems, Center of Energy, Austrian Institute of Technology for their support and providing appropriate data-sets. Authors would also like to thank the partners of iWPP-Flex project for providing the nonlinear thermal building models.

References

[1] A. D. Giorgio, L. Pimpinella, and F. Liberati, "A model predictive control approach to the load shifting problem in a household equipped with an energy storage unit," in *2012 20th Mediterranean Conference on Control Automation (MED)*, Jul. 2012, pp. 1491–1498.

[2] C. Chen, J. Wang, Y. Heo, and S. Kishore, "MPC-Based Appliance Scheduling for Residential Building Energy Management Controller," *IEEE Transactions on Smart Grid*, vol. 4, no. 3, pp. 1401–1410, Sep. 2013.

[3] C. R. Touretzky and M. Baldea, "Model reduction and nonlinear MPC for energy management in buildings," in *2013 American Control Conference*, Jun. 2013, pp. 461–466.

[4] J. A. Momoh, F. Zhang, and W. Gao, "Optimizing renewable energy control for building using model predictive control," in *2014 North American Power Symposium (NAPS)*, Sep. 2014, pp. 1–6.

[5] S. Agheb, X. Tan, and D. H. K. Tsang, "Model predictive control of integrated room automation considering occupants preference," in *2015 IEEE International Conference on Smart Grid Communications (SmartGridComm)*, Nov. 2015, pp. 665–670.

[6] O. Alrumayh and K. Bhattacharya, "Model predictive control based home energy management system in smart grid," in *2015 IEEE Electrical Power and Energy Conference (EPEC)*, Oct. 2015, pp. 152–157.

[7] S. Hanif, D. F. R. Melo, M. Maasoumy, T. Massier, T. Hamacher, and T. Reindl, "Model predictive control scheme for investigating demand side flexibility in Singapore," in *2015 50th International Universities Power Engineering Conference (UPEC)*, Sep. 2015, pp. 1–6.

[8] Š. Kozák, A. Pytel, and P. Drahoš, "Application of hybrid predictive control for intelligent buildings," in *2015 20th International Conference on Process Control (PC)*, Jun. 2015, pp. 203–208.

[9] D. Oliveira, E. M. G. Rodrigues, R. Godina, T. D. P. Mendes, J. P. S. Catalão, and E. Pouresmaeil, "Enhancing home appliances energy optimization with solar power integration," in *IEEE EUROCON 2015 - International Conference on Computer as a Tool (EUROCON)*, Sep. 2015, pp. 1–6.

[10] R. Godina, E. M. G. Rodrigues, E. Pouresmaeil, and J. P. S. Catalão, "Home HVAC energy management and optimization with model predictive control," in *2017 IEEE International Conference on Environment and Electrical Engineering and 2017 IEEE Industrial and Commercial Power Systems Europe (EEEIC / I CPS Europe)*, Jun. 2017, pp. 1–5.

[11] H. Nagpal, B. Basu, and A. Staino, "Economic model predictive control of building energy systems in cooperative optimization framework," in *2018 Indian Control Conference (ICC)*, Jan. 2018, pp. 306–311.

[12] B. Rao, F. Kupzog, and M. Kozek, "Phase Balancing Home Energy Management System Using Model Predictive Control," *Energies*, vol. 11, no. 12, p. 3323, Nov. 2018.

[13] B. V. Rao, F. Kupzog, and M. Kozek, "Three-Phase Unbalanced Optimal Power Flow Using Holomorphic Embedding Load Flow Method," *Sustainability*, vol. 11, no. 6, p. 1774, Jan. 2019.